journal homepage: www.intl.elsevierhealth.com/journals/cmpb

Prediction of externally applied forces to human hands using frequency content of surface EMG signals

Yunus Ziya Arslan[a,*], *Mehmet Arif Adli*[b], *Aydin Akan*[c], *Mehmet Baris Baslo*[d]

[a] *Department of Mechanical Engineering, Faculty of Engineering, Istanbul University, 34320 Avcilar, Istanbul, Turkey*
[b] *Department of Mechanical Engineering, Faculty of Engineering, Marmara University, 34722 Kadikoy, Istanbul, Turkey*
[c] *Department of Electrical and Electronics Engineering, Faculty of Engineering, Istanbul University, 34320 Avcilar, Istanbul, Turkey*
[d] *Department of Neurology, Istanbul School of Medicine, Istanbul University, 34093 Capa, Istanbul, Turkey*

ARTICLE INFO

Article history:
Received 17 November 2008
Received in revised form
31 July 2009
Accepted 23 August 2009

Keywords:
Higher order frequency moments
Surface electromyography
Externally applied forces
Human hand

ABSTRACT

In this work, a new signal processing method was proposed in order to predict externally applied forces to human hands by deriving a relationship between the surface electromyographic (SEMG) signals and experimentally known forces. This relationship was investigated by analyzing the spectral features of the SEMG signals. SEMG signals were recorded from three subjects during isometric contraction and from another three subjects during anisometric contraction. In order to determine force–SEMG signal relationship, higher order frequency moments (HOFMs) of the signals were calculated and used as characterizing features of SEMG signals. Subsequently, artificial neural networks (ANN) with backpropagation algorithm were trained by using the HOFMs. Root mean square difference (RMSD) between the actual and predicted forces was calculated to evaluate force prediction performance of the ANN. In addition to RMSD, cross-correlation coefficients between actual and predicted force time histories were also calculated for anisometric experiment results. The RMSD values ranged from 0.34 and 0.02 in the isometric contraction experiments. In the anisometric contraction tests, RMSD results were between 0.23 and 0.09 and cross-correlation coefficients ranged from 0.91 to 0.98. In order to compare the performance of the HOFMs with a widely used EMG signal processing technique, root-mean-squared (RMS) values of the EMG signals were also calculated and used to train the ANN as another characterizing feature of the signal. Predicted forces using HOFMs technique were in general closer to the actual forces than those of obtained by using RMS values. The results indicated that the proposed signal processing method showed an encouraging performance for predicting the forces applied to the human hands, and the spectral features of the EMG signal might be used as input parameter for the myoelectric controlled prostheses.

1. Introduction

Numerous studies have investigated the relationship between the surface electromyographic (SEMG) signals [1] and externally applied forces to the human hand [2–4]. One of the main reasons for determining this relationship is to predict the forces exerted by human hand more accurately and hence improve the performance of myoelectric controlled prostheses and artificial limbs.

* *Corresponding author*. Tel.: +90 212 473 70 70/17748: fax: +90 212 473 71 80.
E-mail address: yzarslan@istanbul.edu.tr (Y.Z. Arslan).

0169-2607/$ – see front matter
doi:10.1016/j.cmpb.2009.08.005

Using EMG signals for controlling the prosthesis can give natural movement abilities to the amputees. Therefore, various EMG controlled prostheses and exoskeleton robots were developed for people amputated from upper [5–9] and lower extremities [10] to facilitate the activities of daily living. Operating system principles of the myoelectric controlled prostheses are generally based on the detection of the amputee's intended movement by using SEMG signal. In order to convert the muscle activity levels of human subject into the prosthetic actions, first SEMG stimulus is received by sensors and then an appropriate movement orientation and force production are regulated by a mechanical control system [11]. EMG controlled prosthetic hands having multi-degrees of freedom (DOF), which can distinguish the forearm motion patterns from EMG signals using artificial neural networks (ANN), have been developed in laboratory conditions [12,13]. However, today only single DOF EMG controlled prostheses are generally used in daily activities by amputees [5]. Morita et al. [6] proposed a control method for a prosthetic hand, which could estimate joint torque from the EMG signals using neural networks. Their proposed method provided output for the control signal of each joint in parallel. They concluded that there was a possibility to realize more complicated motions in comparison with the conventional method classifying each motion pattern discretely from EMG signals using the neural networks.

In addition to prosthesis control, much work has been done concerning the EMG signal–force applications including musculoskeletal modeling [14–20] and ergonomics [21]. Unlike our research, the main goal of those musculoskeletal modeling studies is to predict the individual muscle forces. Furthermore, a lot of research on the estimation of elbow joint torques from EMG signals was also carried out [22–25]. In some of these studies, the ANN were used to derive a complex relationship between EMG and force or joint torque [17,23,24]. It is deduced from these studies that ANN might be used to predict forces based on EMG signals.

Various techniques have been used to characterize EMG signals in frequency domain [26–28]. Power spectral density (PSD) of the EMG activity can be estimated using classical methods (periodogram and Blackman–Tukey estimators) or parametric model methods (autoregressive, moving average, autoregressive moving average) [26]. The key issue to be taken into account while processing a signal using above methods is to avoid the distortion of the signal features, which involve the functional properties of the corresponding muscle.

The present study describes a series of experiments where we applied higher order statistical moments [29] of the PSD of the SEMG activity to predict externally applied forces to the human hands. In the experiments, SEMG signals were recorded from the proximal muscles of the upper extremity during isometric and anisometric contractions. Higher order frequency moments (HOFMs) of the signals were calculated as characterizing features. In the literature, probably the most widely used signal processing method for EMG signal is root-mean-squared (RMS) analysis [1]. Therefore, in order to evaluate the characterizing performance of the HOFMs, RMS values of the EMG signals were calculated. An artificial neural network was trained and validated by using HOFMs and RMS features separately. Finally, the forces predicted using these two methods were compared with the actual forces.

2. Materials and methods

2.1. *Experimental set-up and procedure*

SEMG signal recordings were carried out during two types of muscle contraction; isometric (also isotonic) and force-varying anisometric contractions. Experiments were implemented by six right-handed healthy male subjects ranging from ages 25 to 35. The SEMG signals were recorded from three subjects during isometric contraction and from another three subjects during anisometric contraction. The subjects were given sufficient information about the experiments and their informed consents were taken.

The control process of the myoelectric controlled prostheses must have on-line adaptation ability to a variety of movement tasks of each human subject [8]. Since the EMG signal is a biologically generated signal, it is difficult to obtain the same EMG signal for the same motion even from the same person. In addition to this, the level of the EMG signals might be much different between subjects. These complex properties of the EMG signals require specific and individual control process designs for each amputee's prosthesis. Therefore, in this study, instead of including a lot of subjects and making a great effort to gather EMG signals from a large number of people, it was preferred to collect many EMG data from a small set of subjects. In this way, it was aimed to focus our attention on consistent and reliable force estimation from EMG signals specific to the individual.

A vast majority of patients who require upper limb prosthesis had undergone amputations from distal joints to elbow [30]. The upper limb amputations from the level of elbow to shoulder are at a very small rate of 7–8%. Therefore, most amputated people can still control the muscles of the proximal part of the upper body. Since the main motivation of this study was to use the SEMG signals as an input for the control process of myoelectric controlled prostheses, signals were acquired simultaneously from the muscles of the proximal part of the upper body, i.e. biceps brachii, triceps brachii, pectoralis major and trapezius. Considering the position of the arm in the experiments, these four muscles were among the most actively contracting muscles of the proximal part of the upper body.

2.1.1. *Isometric measurements*

In order to evaluate the relationship between increasing forces on the muscle activation, the following experiment was carried out.

The right forearm was placed on a grass surfaced table parallel to the coronal plane, transverse plane and ground; also it was stabilized at flexed position with 90° while the forces were applied. The flexion and abduction angles of the right upper arm were 45° and 0°, respectively. To decrease the dry friction between the skin surface of the forearm and the table, a special silk fabric with low dry friction was used. During isometric contractions of the right arm 14 different force values had to be reached. The forces were varied between 10 N and 75 N with 5 N increments and measurements were taken for 3 s and repeated 50 times at each force level. In order to minimize the effect of the muscle fatigue, which could negatively affect

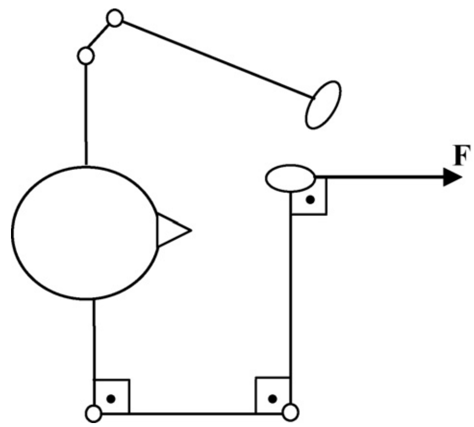

Fig. 1 – The positions of the subject's shoulder and arm from top view.

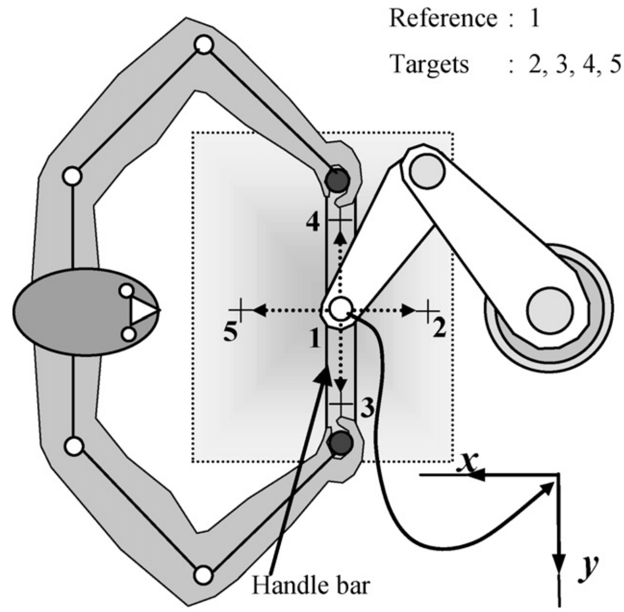

Fig. 2 – Top view of the experimental set-up used to carry out bi-manual manipulation.

the classification of the signals, the subjects were asked to rest along between the successive contractions. Subjects were put on rest until the tremor activity seen on EMG, which is one of the indicators of fatigue, disappeared and subjects felt themselves in non-fatiguing condition. Right forearm and hand were held in a straight line by using a support brace wrapped around wrist. Force was applied to human hand by means of a pulley mechanism such that the direction of the force was perpendicular to the longitudinal axis of forearm. The positions of the shoulder and arms during the experiments are shown in Fig. 1.

The SEMG recording system used in the experiments was Key Point version 5.03, Physiomed, Denmark (common mode rejection ratio >100 dB, input impedance = 1000 MΩ, signal-to-noise ratio = 0.6 μV). The electrodes used for recordings were Ag/AgCl discs with 10 mm diameter. In order to achieve a good contact between the electrodes and muscles, alcohol was applied to cleanse skin and a special conducting gel was used. Recorded SEMG signals were applied to a bandpass filter with 20 Hz lower and 250 Hz upper frequency cut-offs. The sampling frequency of the signals was 500 Hz.

2.1.2. *Anisometric measurements*

The set-up used for carrying out the experiments for anisometric measurements is shown in Fig. 2. The experimental set-up consisted of a direct drive SCARA type robot manipulator, which has three DOF. A handle bar was mounted at the tip of the manipulator. Interaction forces between the human hands and the handlebar and between the manipulator and the handlebar were measured by two six-axis force/torque sensors (NITTA Corporation, Japan, 500 Hz sample frequency) with accuracy of $\pm 10g$.

The robot manipulator consists of three links which were all connected by rotational joints. The distance between the robot base and the subject hand was set to 0.75 m, a distance enough for a comfortable workspace for both the subject and the robot manipulator. The distance between the reference point (point 1, Fig. 2) and the subject was 0.43 m. The robot arm tip was connected to a 40 cm handlebar at its center by a revolute joint. In this way the handlebar was coupled to the robot arm and became its actively controlled third link. At the reference position (1), the robot arm tip, hence the handlebar was at static equilibrium which was maintained by controlling the robot arm. The robot arm was controlled using task space stiffness control. That is, as the handlebar is moved from reference point to the specified targets, the robot arm reacts to the motion depending on the specified task space stiffness parameters.

During the experiment the subject was seated in front of a horizontal table and firmly grasped two handles on the handlebar. Shoulder movement of the subject was restrained by a harness. Wrists were immobilized by putting solid plates around the wrists so that each arm can be treated as a two-link manipulator consists of shoulder and elbow. Flexion angle of the shoulder at the neutral position was 90° and abduction angle of the shoulder changed according to the length of the forearm and upper arm of the subjects. The handlebar has three degrees of motion freedom (two translations and a rotation) and allows a floating motion in the horizontal plane formed by the subject's arms. Four different target sets, and a reference position were specified on the table (Fig. 2). Two target sets were used for the motion along the anterior–posterior axis and the other two were used for the motion along the medio-lateral axis. These motions were named as:

$$1 \to 2 : \text{forward}, \quad 1 \to 3 : \text{rightward}, \quad 1 \to 4 : \text{leftward},$$
$$1 \to 5 : \text{backward}.$$

The subject was asked to move the handlebar from the reference point to the specified target. Each motion from the reference point to the specified target was divided into three phases, i.e. *proceed* phase, *maintain* phase and *retreat* phase. Using a metronome, the subject was instructed by a tone signal (a beep) to make an advancing motion of δ = 50 mm towards the visually guided desired target, and *maintain* the handlebar there for 4 s until the next tone, and then make the retreating

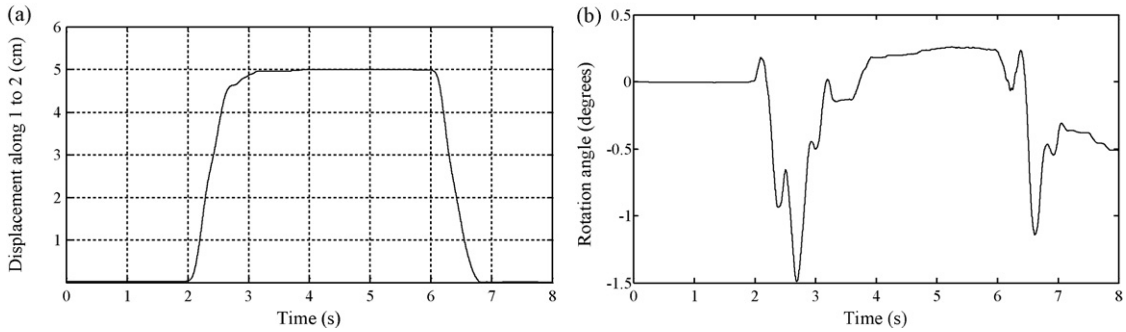

Fig. 3 – (a) Displacement–time profile of the revolute joint of the handle bar along 1 → 2 (forward phase) and (b) angle change around revolute joint during pushing movement. Negative angle values denote rotation in the clockwise direction.

motion back to the reference position. In addition to the *maintain* phase, data were also collected for 2 s before the *proceed* and after the *retreat* phases during which the subject relaxed. *Proceed* and *retreat* phases of the motion were instantaneous and the time elapsed during these phases was in general very short. These motions were repeated 10 times for each subject. The synchronization between EMG and force measurements was done using IO signals between AD converter cards.

In the experiments, position and orientation of the robot arm (robot handle) were measured by the optical encoders mounted on its joints. The position and motion speed of the handlebar were monitored using displacement–time data obtained from these devices. Thus, a probable improper movement pattern would be detected by this way. A representative displacement–time profile of the revolute joint of the handle bar along 1 → 2 direction (forward phase) and angle variation around revolute joint are shown in Fig. 3a and b, respectively. It can be deduced from Fig. 3 that the handlebar motion from reference point to a target point was completed approximately in 1 s and angle variation around revolute joint of the handle bar was less than 2°.

2.2. *Signal processing*

In this study, EMG signals with 3 s (for isometric contraction) and 8 s (for anisometric contraction) time durations were scanned via a sliding and overlapping Hamming window. An EMG signal is generally assumed to be stationary for duration of 500 ms [26]. Hence our observed data were segmented using overlapping windows of 500 ms width. The time interval between the successive windows was 50 ms. Therefore, after the scanning of the signals, 61 segments for isometric contractions and 161 segments for anisometric contractions were obtained.

The power spectra $P(\omega_k)$ of EMG segments were estimated by using periodogram approach [31]. The periodogram estimate of the PSD of a discrete-time signal $x(n)$; $n = 0, 1, \ldots, N-1$, with N samples is given by

$$P(\omega_k) = \frac{1}{N}\left|X(\omega_k)\right|^2, \quad \omega_k = \frac{2\pi}{N}k, \quad k = 0, 1, \ldots, N-1, \qquad (1)$$

where ω_k is discrete frequency and $X(\omega_k)$ denotes the Discrete Fourier Transform (DFT) of $x(n)$.

Power spectrum contains enough information to characterize the EMG signal and it was also used in previous studies [27,28]. However, for a signal of length N, it is required to calculate an N sample power spectral estimate, which means higher number of features and higher computational burden. Instead of the whole power spectrum, using a few features extracted from it will be a computational advantage [32]. In our proposed method, after estimating the power spectrum for the overlapping segments of EMG signal, HOFMs up to fourth order were calculated and used as the characterizing features of the EMG activity. For a discrete-time signal $x(n)$, HOFMs can be calculated as follows:

$$\langle \omega_k^j \rangle = \sum_{k=0}^{N-1} \omega_k^j P(\omega_k), \quad j = 0, 1, \ldots \qquad (2)$$

where, $\langle \omega_k^j \rangle$ is the jth order frequency moment.

In order to evaluate the characterizing performance of the HOFMs, RMS of the windowed signal was also calculated. To have a proper comparison of these analysis techniques operating on the same signal, same windowing features used in HOFMs calculations were chosen for RMS feature calculations.

A representative signal, recorded during anisometric contraction, its RMS features, and one of the spectral moments of this signal used for training, that is, the second order moments are presented together in Fig. 4. In order to make a proper comparison in the figure, EMG signal, RMS value, and frequency

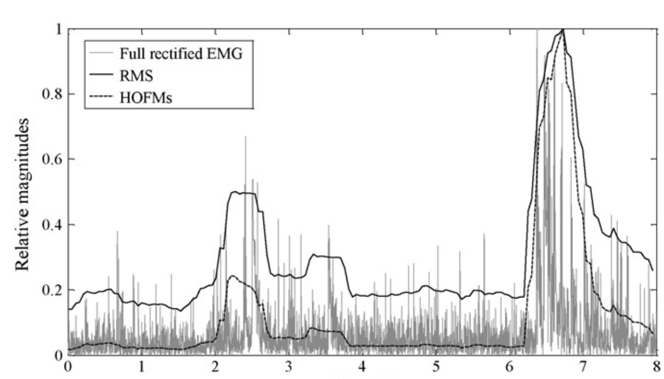

Fig. 4 – A representative EMG signal and its new forms, i.e. RMS features and second order spectral moments.

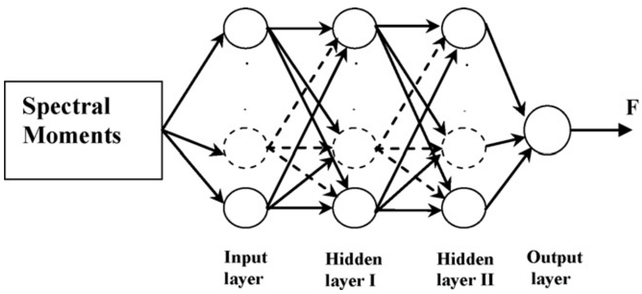

Fig. 5 – Artificial neural networks model.

moments were normalized by their respective maximum values.

2.3. Artificial neural networks

The ANN were trained using spectral moments and RMS values of the overlapping EMG segments separately for estimating the applied forces. The ANN had one input layer, two hidden layers, and one output layer (Fig. 5). Learning process of the ANN occurs at the synaptic junctions between the neurons of the input layer and the neurons of the output layer. The input array, which represents values of categorical input fields, was constituted from spectral moments up to fourth order and RMS values; target was constituted from the forces applied to human hands. In order to improve the learning performance of the ANN, force values used in the target set were normalized to a range between 0 and 1.

Half of the measurements of each subject were randomly chosen and used to train the network and the other half was fed into the ANN for validation. Then, training and test sets were switched for cross-validation and performance test was repeated.

In the network model, one input layer, two hidden layers, and one output layer having 61, 10, 5, and 1 neurons were used for isometric trials, respectively. The only difference between network models used for the isometric and anisometric experiments was the neuron number of the input layer, namely 161 neurons were used in anisometric trials. The number of the neurons used in the hidden layers were determined adaptively, i.e. tuning the number of neurons by training the ANN a few more times until obtaining the satisfactory ones [33]. Log-sigmoid transfer function was employed as the transfer function, which is used for calculations between the neurons during the training process. Backpropagation feedforward was used as the training algorithm. Backpropagation algorithm is an extension of the Least Mean Square learning algorithm which is widely used in adaptive signal processing. In this algorithm the weights are adjusted at each step to reduce the gradient of the cost function that is the mean squared error [34]. Number of the epoch was chosen 500 for the learning stage of the network.

2.4. Evaluation of force predictions

In order to evaluate the force predictions, the root mean square difference (RMSD) and the cross-correlation coefficient (γ) between the actual and predicted forces, which are commonly used as evaluation criteria for the force prediction applications, were calculated [23,35].

The RMSD between the actual $f_x(n)$ and predicted $f_y(n)$ forces is obtained from the following equation [23]:

$$\mathrm{RMSD} = \sqrt{\frac{\sum_n (f_y(n) - f_x(n))^2}{\sum_n (f_x(n))^2}} \tag{3}$$

In our investigation, if the value of RMSD is 0.01, it means that the predicted force has about 1% mean error from the actual forces. Furthermore, the observed differences of RMSD values of the HOFMs and RMS analyses were evaluated from the viewpoint of statistics by means of ANOVA. The differences were evaluated at a level of significance of 0.05.

Cross-correlation coefficient γ is a measure of the similarity between two curves [35] and calculated as follows:

$$\gamma = \frac{C_{xy}(0)}{\sqrt{C_{xx}(0)}\sqrt{C_{yy}(0)}} \tag{4}$$

where $C_{xy}(0)$ is the cross-covariance of f_x and f_y, $C_{xx}(0)$ and $C_{yy}(0)$ are the autocovariance of f_x and f_y, respectively and the lag is taken as 0. In our observation, if the cross-correlation coefficient is 0, then it is deduced that the predicted and actual forces are uncorrelated. Equivalent force data sets have a cross-correlation coefficient of 1.

3. Results

3.1. Force predictions in isometric contractions

For each applied force value, 50 SEMG signal samples were taken, and the force was predicted by the proposed method using each signal. Then the mean and standard deviations (SD) were calculated by using the whole predicted force data. The comparison of the mean and SD of the forces obtained by RMS and HOFMs techniques, for all subjects in the isometric contraction tests are presented in Fig. 6.

For a detailed quantitative evaluation of the force prediction performance, RMSD values between the actual forces and predicted forces are given in Table 1. It is seen from Table 1 that the RMSD values obtained from HOFMs ranged between 0.34 and 0.02. Means of the RMSD values obtained from HOFMs for all applied force levels were 0.07, 0.16 and 0.10 for subjects I, II and III, respectively. The RMSD values obtained from RMS analysis ranged between 0.34 and 0.05; and means of the RMSD values obtained from RMS analysis for all applied force levels were 0.10, 0.16 and 0.11 for subjects I, II and III, respectively.

3.2. Force predictions in anisometric contractions

A typical example of the predicted force time history results of a subject for the anisometric contraction experiments is shown in Fig. 7. In the figure, predicted forces as well as the actual forces are seen for the various target sets, i.e. the forward, rightward, leftward and backward motions. These forces are actually the reaction forces that the robot arm shows

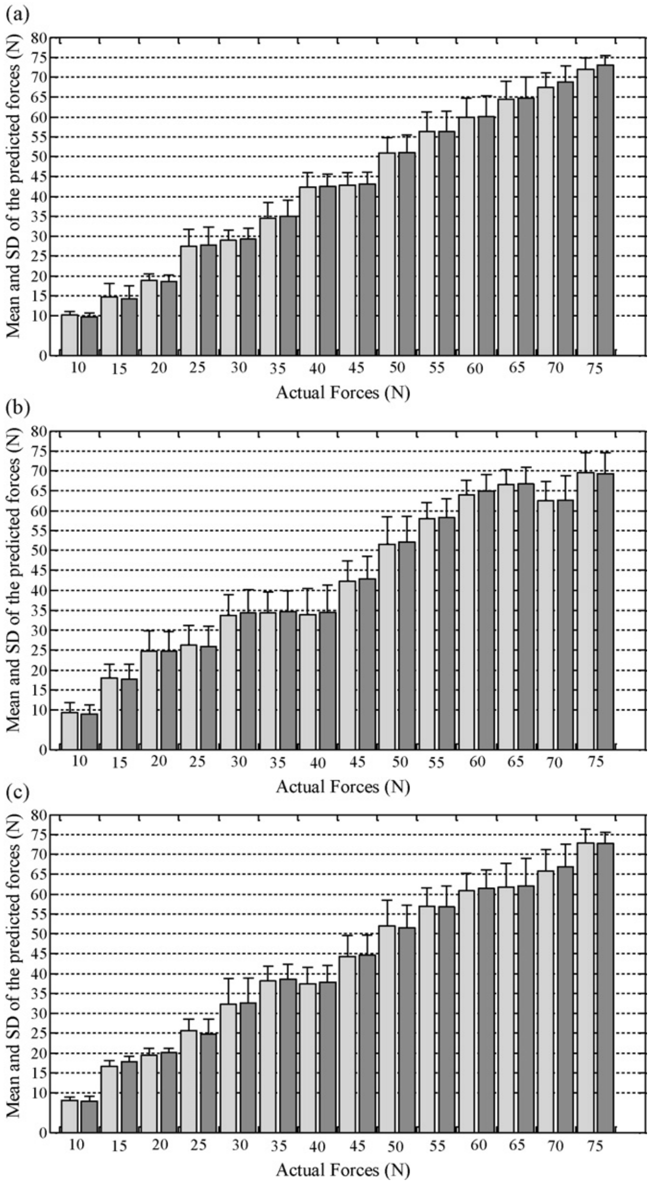

Fig. 6 – Mean and SD of the predicted forces for (a) subject I, (b) subject II and (c) subject III. Light grey and dark grey bars denote the predicted forces obtained by RMS and HOFMs features, respectively.

against the motion. The force values depend on both the specified task space stiffness parameters and the inherent structural stiffness of the robot arm.

The RMSD values and cross-correlation coefficients (γ) are given for anisometric experiments in Tables 2 and 3. Each value given in these tables shows the mean of the test results obtained using RMS and HOFMs features, respectively. The RMSD values and the cross-correlation coefficients obtained using HOFMs features ranged from 0.23 to 0.09 and from 0.91 and 0.98, respectively. The RMSD values and the cross-correlation coefficients obtained using RMS features ranged from 0.24 to 0.09 and from 0.93 and 0.99, respectively.

4. Discussion

In this study, in order to predict the externally applied forces to human hands, the SEMG signal–force relationship was investigated by analyzing the spectral features of the SEMG activity. To achieve this goal, SEMG signals were recorded from four proximal muscles of the upper body during the isometric and anisometric contractions of the muscles. Contractions during experiments were non-fatiguing. Furthermore, motion capability of the arms was partly restricted.

In order to characterize SEMG signals, HOFMs of the signals up to fourth order were calculated. HOFMs enabled us to use very few features instead of the whole frequency content of the signal and hence to decrease the computational cost. Then, ANN were used to obtain a relationship between the spectral features of the signals and externally applied forces. The ANN provided force predictions from SEMG signals. The RMSD and the cross-correlation coefficients between the actual and predicted forces were calculated to evaluate the force prediction performance of the ANN. The RMSD values obtained in the isometric contraction experiments were below 0.34. Especially, most of these values were below 0.10 for the large force values which were over 55 N. Furthermore, means of the RMSD values for all applied force levels were 0.07, 0.16 and 0.10 for subjects I, II and III, respectively. In addition to isometric trials, an encouraging performance was achieved in anisometric experiments such that, RMSD values ranged from 0.09 to 0.23 and the cross-correlation coefficients ranged between 0.91 and 0.98.

In order to test the performance of the HOFMs in terms of capability of characterizing the EMG signal, RMS features of the signal were also calculated and subjected to the same ANN process used for the HOFMs. The maximum RMSD value between the predicted and actual forces was 0.34 which was equal to the one obtained using HOFMs in the isometric task experiments. It is seen from Table 1 that most of the RMSD values obtained using RMS features were higher than those obtained from the HOFMs. The means of the RMSD values obtained using RMS features were higher than those obtained using HOFMs for subjects I and III. The means of the RMSD values obtained using HOFMs and RMS features were equal for subject II.

In the anisometric contraction experiments, it was found that most of the error values of the HOFMs features were less than those obtained by RMS features (Tables 2 and 3). In addition, comparing the cross-correlation coefficients of these two features, it was realized that the characterization performance of the HOFMs features was almost equal to one of the RMS features. Despite HOFMs showed a slightly better performance than RMS, a statistically significant difference between the RMDS values of both techniques was found neither in the isometric nor in the anisometric experiments for any subjects ($p > 0.05$).

Although the HOFMs showed promising performance in characterization of EMG signals, the major contribution of this study does not only stem from the prediction results. In this study it was demonstrated that spectral features of a myoelectric signal could also be used to analyze the force–signal relationship. In Fig. 4 it can be observed that the time his-

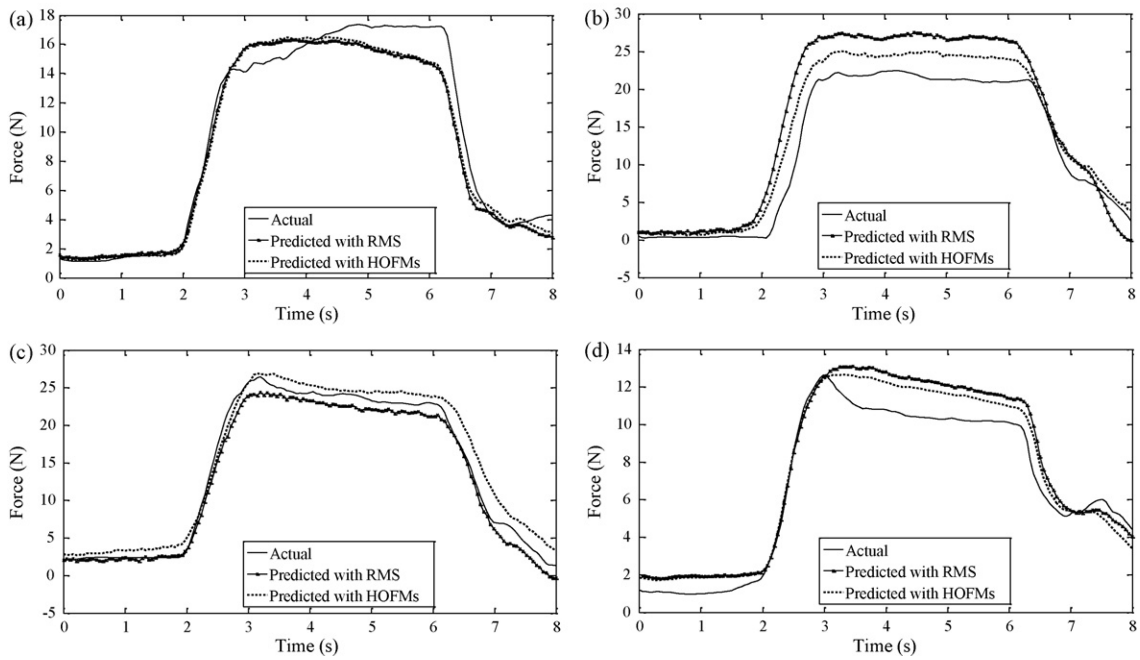

Fig. 7 – A sample result of a subject for comparison of the predicted forces with the actual forces for (a) 1 → 2 forward motion, (b) 1 → 3 rightward motion, (c) 1 → 4 leftward motion and (d) 1 → 5 backward motion.

Table 1 – Force estimation performance results of both the RMS and HOFMs features for isometric contraction experiments.

Forces	Subject I RMSD		Subject II RMSD		Subject III RMSD	
	RMS	HOFMs	RMS	HOFMs	RMS	HOFMs
10 N	0.09	0.07	0.25	0.29	0.20	0.24
15 N	0.22	0.21	0.29	0.30	0.14	0.19
20 N	0.10	0.08	0.34	0.34	0.07	0.05
25 N	0.19	0.17	0.20	0.16	0.11	0.10
30 N	0.09	0.06	0.20	0.21	0.22	0.21
35 N	0.11	0.09	0.14	0.12	0.13	0.12
40 N	0.10	0.07	0.22	0.21	0.12	0.10
45 N	0.08	0.06	0.12	0.11	0.11	0.10
50 N	0.08	0.07	0.14	0.14	0.13	0.10
55 N	0.09	0.07	0.09	0.10	0.09	0.07
60 N	0.08	0.06	0.09	0.10	0.07	0.06
65 N	0.07	0.04	0.06	0.06	0.10	0.08
70 N	0.06	0.04	0.12	0.11	0.09	0.07
75 N	0.05	0.02	0.10	0.10	0.05	0.04
	0.10	0.07	0.16	0.16	0.11	0.10

The last row indicates the mean values of the related columns.

Table 2 – Force estimation performance results of the RMS features for anisometric contraction experiments.

Subjects	1 → 2 forward		1 → 3 rightward		1 → 4 leftward		1 → 5 backward	
	RMSD	γ	RMSD	γ	RMSD	γ	RMSD	γ
Subject IV	0.12	0.98	0.14	0.98	0.16	0.97	0.16	0.97
Subject V	0.12	0.98	0.13	0.98	0.14	0.97	0.22	0.94
Subject VI	0.21	0.94	0.09	0.99	0.17	0.97	0.24	0.93

Table 3 – Force estimation performance results of the HOFMs features for anisometric contraction experiments.

Subjects	1 → 2 forward		1 → 3 rightward		1 → 4 leftward		1 → 5 backward	
	RMSD	γ	RMSD	γ	RMSD	γ	RMSD	γ
Subject IV	0.10	0.98	0.12	0.98	0.14	0.97	0.14	0.98
Subject V	0.11	0.98	0.11	0.98	0.17	0.96	0.21	0.94
Subject VI	0.23	0.91	0.09	0.98	0.17	0.96	0.21	0.94

tory profiles of the RMS and HOFMs features are similar for the same signal. In literature, spectral analysis of the EMG signal has in general been carried out to quantify muscle fatigue [26,36,37]. However in this research, spectral analysis was performed to predict the applied forces. In the light of this study's findings, one can consider combining the information extracted from EMG signals in both frequency- and time-domain for prosthesis control. Furthermore, using either the RMS or the HOFMs as features of the EMG signal itself has the advantage of reducing the data size that will be used in the training of ANN, and thus reducing the computational cost. For example in our anisometric contraction experiments, for an EMG signal segment of 4000 samples, ANN with only 161 input neurons were sufficient whereas 4000 neuron would have been used if we trained the whole EMG signal instead of the features.

The validation performance of the ANN can be improved by tuning the number of design variables such as the neurons, layers and number of epochs. However, it is not possible to propose a standard ANN design for training the EMG signal efficiently.

The arm movements performed in the experiments covered a small range of possible movements observed in every day arm activities. According to the von Tscharner and Nigg, power spectra of EMG signal depends primarily on muscles task [38]. Hence, a more comprehensive evaluation of the proposed technique's performance may be done by extending the analysis to a larger range of experimental tasks to simulate all possible arm movements.

5. Conclusions

It can be concluded from the prediction results that HOFMs can be used to characterize the SEMG signals. The proposed method enabled to predict the externally applied forces to the human hands with a promising performance. In the light of findings, HOFMs are recommended to use as input signals in the control processes of active arm prostheses for patients with amputated arms from the elbow. Furthermore, it is also suggested that higher order joint time–frequency moments, instead of power spectral moments, may also be used to classify SEMG signals which are non-stationary in nature. Thus, time-varying properties of the signals may be tracked better, which is considered in our ongoing research.

Acknowledgments

The experiments were carried out in the Department of Neurology, Istanbul University and in the Laboratory of Bio-Mimetic Control Research Center, RIKEN, Japan, where the second author was affiliated with. The authors would like to acknowledge the support provided by Department of Neuroscience and Laboratory of Bio-Mimetic Control Research Center. This work was partially supported by The Research Fund of The University of Istanbul, project numbers: UDP-3826/25052009 and BYP-3705/15052009.

REFERENCES

[1] J.V. Basmajian, C.J. De Luca, Muscles Alive. Their Function Revealed by Electromyography, Williams & Wilkens, Baltimore, 1985.

[2] Y. Kurita, M. Tada, Y. Matsumoto, T. Ogasawara, Simultaneous measurement of the grip/load force and the finger EMG: effects of the grasping condition, in: Proceedings of IEEE International Workshop on Robot and Human Interactive Communication, Berlin, 2002, pp. 217–222.

[3] D. Roman-Liu, T. Tokarsky, EMG of arm and forearm muscle activities with regard to handgrip force in relation to upper limb location, Acta of Bioengineering and Biomechanics 4 (2) (2002) 33–48.

[4] J.M. Eklund, F. Mobasser, K. Hashtrudi-Zaad, Hand force estimation using fast orthogonal search, in: Proceedings of 26th Annual International Conference of the IEEE EMBS, San Francisco, 2004, pp. 695–698.

[5] S. Morita, K. Shibata, X.Z. Zheng, K. Ito, Prosthetic hand control based on torque estimation from EMG signals, in: Proceedings of IEEE International Conference on Intelligent Robots and Systems, Takamatsu, 2000, pp. 389–394.

[6] S. Morita, T. Kondo, K. Ito, Estimation of forearm movement from EMG signal and application to prosthetic hand control, in: Proceedings of IEEE International Conference on Robotics & Automation, Seoul, 2001, pp. 3692–3697.

[7] K. Kuribayashi, K. Okimura, T. Taniguchi, A discrimination system using neural network for EMG-controlled prosthesis, in: Proceedings of IEEE International Workshop on Robot and Human Communication, Tokyo, 1992, pp. 63–68.

[8] K. Kiguchi, K. Iwami, M. Yasuda, K. Watanabe, T. Fukuda, An exoskeletal robot for human shoulder joint motion assist, IEEE/ASME Transactions on Mechatronics 8 (1) (2003) 125–135.

[9] K. Ito, T. Tsuji, A. Kato, M. Ito, EMG pattern classification for a prosthetic forearm with three degrees of freedom, in: Proceedings of IEEE International Workshop on Robot and Human Communication, Tokyo, 1992, pp. 69–74.

[10] C. Fleischer, A. Wege, K. Kondak, G. Hommel, Application of EMG signals for controlling exoskeleton robots, Biomedizinische Technik 51 (5–6) (2006) 314–319.

[11] A. Herrera, M. Adjouadi, M. Ayala, An Integrated Design for a Myoelectrically-based Writing Module for a Controlled Prosthesis, Lecture Notes on Computer Science, Springer, Berlin/Heidelberg, 2006, pp. 926–934.

[12] B. Hudgins, P. Parker, N. Scott, A new strategy for multifunction myoelectric control, IEEE Transactions on Biomedical Engineering 40 (1) (1993) 82–94.

[13] K.A. Farry, I.D. Walker, R.G. Baraniuk, Myoelectric teleoperation of a complex robotic hand, IEEE Transactions on Robotics and Automation 12 (5) (1996) 775–788.

[14] L.J. van Ruijven, W.A. Weijs, A new model for calculating muscle forces from electromyograms, European Journal of Applied Physiology 61 (5–6) (1990) 479–485.
[15] G.L. David, T.F. Besier, An EMG-driven musculoskeletal model to estimate muscle forces and knee joint moments in vivo, Journal of Biomechanics 36 (2003) 765–776.
[16] T.S. Buchanan, D.G. Lloyd, K. Manal, T.F. Besier, Neuromusculoskeletal modeling: estimation of muscle forces and joint moments and movements from measurements of neural command, Journal of Applied Biomechanics 20 (4) (2004) 367–395.
[17] M.M. Liu, W. Herzog, H.H.C.M. Savelberg, Dynamic muscle force predictions from EMG: an artificial neural network approach, Journal of Electromyography and Kinesiology 9 (1999) 391–400.
[18] D. Staudenmann, I. Kingma, D.F. Stegeman, J.H. van Dieen, Towards optimal multi-channel EMG electrode configurations in muscle force estimation: a high density EMG study, Journal of Electromyography and Kinesiology 15 (2005) 1–11.
[19] J.J. Woods, B. Bigland-Ritchie, Linear and non-linear surface EMG/force relationship in human muscles. An anatomical/functional argument for the existence of both, American Journal of Physical Medicine 62 (6) (1983) 287–299.
[20] J. Perry, G.A. Bekey, EMG-force relationship in skeletal muscle, Critical Reviews in Biomedical Engineering 7 (1) (1981) 1–22.
[21] M.J.M. Hoozemans, J.H. van Dieen, Prediction of handgrip forces using surface EMG of forearm muscles, Journal of Electromyography and Kinesiology 15 (4) (2005) 358–366.
[22] E.A. Clancy, N. Hogan, Relating agonist-antagonist electromyograms to joint torque during isometric, quasi-isotonic, nonfatiguing contraction, IEEE Transactions on Biomedical Engineering 44 (10) (1997) 1024–1028.
[23] J.J. Luh, G.C. Chang, C.K. Cheng, J.S. Lai, T.S. Kuo, Isokinetic elbow joint torques estimation from surface EMG and joint kinamatic data: using an artificial neural network model, Journal of Electromyography and Kinesiology 9 (3) (1999) 173–183.
[24] T. Uchiyama, T. Bessho, K. Akazawa, Static torque-angle relation of human elbow joint estimated with artificial neural network technique, Journal of Biomechanics 31 (6) (1998) 545–554.
[25] E.A. Clancy, O. Bida, D. Rancourt, Influence of advanced electromyogram (EMG) amplitude processors on EMG-to-torque estimation during constant-posture, force-varying contractions, Journal of Biomechanics 39 (2006) 2690–2698.
[26] A. Georgakis, L.K. Stergioulas, G. Giakas, Fatigue analysis of the surface EMG signal in isometric constant force contractions using the averaged instantaneous frequency, IEEE Transactions on Biomedical Engineering 50 (2) (2003) 262–265.
[27] M. Vuskovic, S. Du, Spectral moments for feature extraction from temporal signals, International Journal of Information Technology 11 (10) (2005) 112–122.
[28] K. Ogino, W. Kozak, Spectrum analysis of surface electromyogram, in: Proceedings of IEEE International Conference on Acoustics, Speech, and Signal Processing, Boston, 1983, pp. 1114–1117.
[29] C.L. Nikias, J.M. Mendel, Signal processing with higher-order spectra, IEEE Signal Processing Magazine 10 (3) (1993) 10–37.
[30] T.R. Dillingham, L.E. Pezzin, E.J. Mac Kenzie, Limb amputation and limb deficiency: epidemiology and recent trends in the United States, Southern Medical Journal 95 (8) (2002) 875–883.
[31] S.M. Kay, Modern Spectral Estimation: Theory and Application, Prentice-Hall, Englewood Cliffs, NJ, 1988.
[32] A. Akan, R.B. Unsal, Time–frequency analysis and classification of temporomandibular joint sounds, Journal of the Franklin Institute Special Issue on Time-Frequency Signal Analysis and Applications 337 (4) (2000) 437–451.
[33] Y.Z. Arslan, M.A. Adli, A. Akan, Investigation of the relationship between EMG signals and the forces applied to human arms, in: Proceedings of 4th International Conference on Electrical and Electronics Engineering, Bursa, 2005, pp. 199–203.
[34] S. Haykin, Neural Networks: A Comprehensive Foundation, second edition, Prentice-Hall, 1999.
[35] H.H.C.M. Savelberg, W. Herzog, Prediction of dynamic tendon forces from electromyographic signals: an artificial neural network approach, Journal of Neuroscience Methods 78 (1–2) (1997) 65–74.
[36] N.A. Dimitrova, G.V. Dimitrov, Interpretation of EMG changes with fatigue: facts, pitfalls, and fallacies, Journal of Electromyography and Kinesiology 13 (2003) 13–36.
[37] D. Farina, R. Merletti, R.M. Enoka, The extraction of neural strategies from the surface EMG, Journal of Applied Physiology 96 (2004) 1486–1495.
[38] V. von Tscharner, B.M. Nigg, Point: spectral properties of the surface EMG can characterize/do not provide information about motor unit recruitment strategies and muscle fiber type, Journal of Applied Physiology 105 (5) (2008) 1671–1673.